COMPDYN 2019
7th ECCOMAS Thematic Conference on
Computational Methods in Structural Dynamics and Earthquake Engineering
M. Papadrakakis, M. Fragiadakis (eds.)
Crete, Greece, 24–26 June 2019

MODELING OF FRP-CONFINEMENT OF LARGE-SCALE RECTANGULAR RC COLUMNS

Konstantinos G. Megalooikonomou [1] and Georgios S. Papavasileiou [2]

[1] Department of Civil and Environmental Engineering
University of Cyprus
P.O. Box 20537, 1687 Nicosia, Cyprus
e-mail: kmegal01@ucy.ac.cy

[2] Department of Construction Technology
Inverness College - University of the Highlands and Islands
1 Inverness Campus, Inverness, IV2 5NA, UK
e-mail: georgios.papavasileiou.ic@uhi.ac.uk

Abstract

One of the main applications of Fiber Reinforced Polymers (FRPs) in construction is in the confinement of reinforced concrete (RC) columns. The performance of FRP-confined concrete in circular columns has been extensively investigated and the efficiency of models available in literature is nowadays considered to be satisfactory. However, the case of FRP-confinement of rectangular RC sections is a more complex problem, the mechanism of which has not yet been adequately described. The aim of this work is to try and simplify the problem by proposing an iterative procedure based on the outcome of 3D FEM analysis run by the authors. An interesting outcome is that the so-called arching effect is never observed: indeed, the unconfined regions are partially confined and provide a certain contribution to the overall strength of the rectangular RC sections. Based on a system of "generalized springs", well-known stress-strain laws and a failure criterion, a simplified mechanical model that gives the stress-strain behaviour of a rectangular RC section confined by FRPs under concentric load is proposed. The algorithm takes into account all parameters available to designers, such as corner rounding radius, stiffness of the FRP and concrete strength, while it can be easily understood and implemented. Its results are found to correlate adequately to recent experimental data yielded by large-scale tests on FRP-confined rectangular RC columns. Finally, in order to further evaluate the performance of this material model, it was implemented in the simulation of a series of experimental tests of FRP-retrofitted square RC columns under cyclic lateral loading simulating earthquake loads and simultaneous constant axial compression, performed by Memon and Sheikh [1]. In particular, all specimens were simulated using nonlinear fiber elements, in which the FRP-confined concrete was modelled using the aforementioned material model. Comparison between the numerical and experimental hysteresis of the column is indicative of the effectiveness of the implemented modelling.

Keywords: Confinement, FRP, Concrete, Rectangular, Model, Stress-Strain Behaviour.

1 INTRODUCTION

The behaviour of fiber reinforced polymer (FRP) - confined concrete in circular columns has been widely studied, and now the efforts of many researchers are directed towards the comprehension of the case of FRP-confined rectangular columns. Here, concrete is non-uniformly confined and the confinement effectiveness is remarkably reduced. In the literature, past approaches have concentrated on dividing the rectangular section in a confined and an unconfined area, based on the idea of possible arching effect between corners. Then, the confined zone is considered to be in a state of uniform biaxial confinement, like in the circular cross section, thus allowing the use of formulas derived for circular columns, while the unconfined zone is considered unaffected. This different behaviour is usually accounted for through so-called effectiveness coefficients, mainly based on geometrical considerations on the relative size of the two different zones. In this study, an alternative approach is attempted, which recognizes, through an iterative procedure based on the outcome of 3D FEM analysis, that the arching effect does not really exist. The unconfined regions are indeed partially confined and contribute, though to a lesser extent with respect to the core, to the total strength of the rectangular sections.

2 NUMERICAL ANALYSIS (FEM)

In a paper of Campione and Miraglia [2] the picture below (Fig. 1a) is reported. The figure is related to the cross-section of a short square column and shows the effective concrete core after FRP failure at the corner. Uneven damage can be observed throughout the section and two different regions can be identified having different confinement stress state. In order to specify the path of the confining stresses and better examine the borders of those regions, a 3D FEM in SAP 2000 [3] (linear range) has been developed (Fig. 1b).

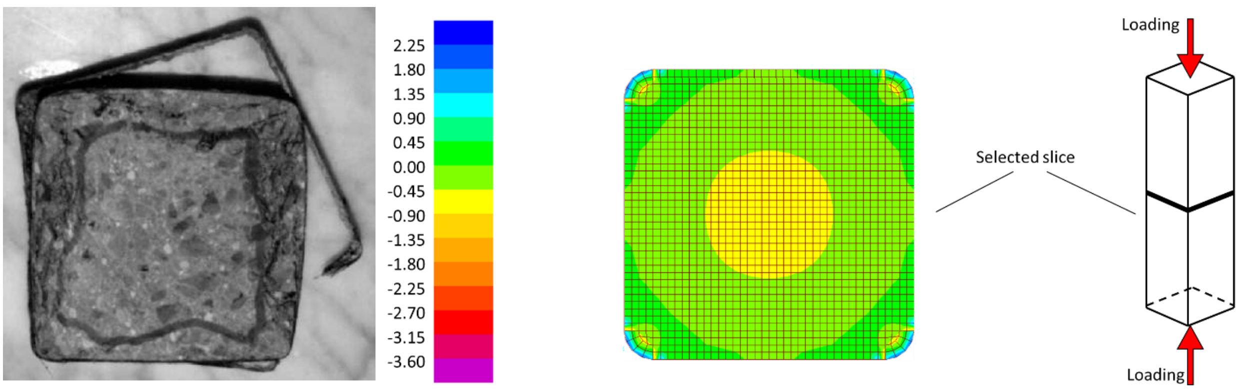

(a) **(b)**

Fig. 1. Cross-section of a short square column: (a) experiment [2], (b) FEM model [4].

From the results obtained from the program, 3D plots were drawn to study the stress field. The next four plots depict different stress fields in a quarter section (100x100 mm). Stresses near the rounded corner are not shown since they represent local stress states. Firstly, the normal stresses parallel to the diagonal are presented and then those in the perpendicular direction, so to better recognize the direction of the confining forces.

Fig. 2 illustrates the confining stresses in a quartile of a square section.

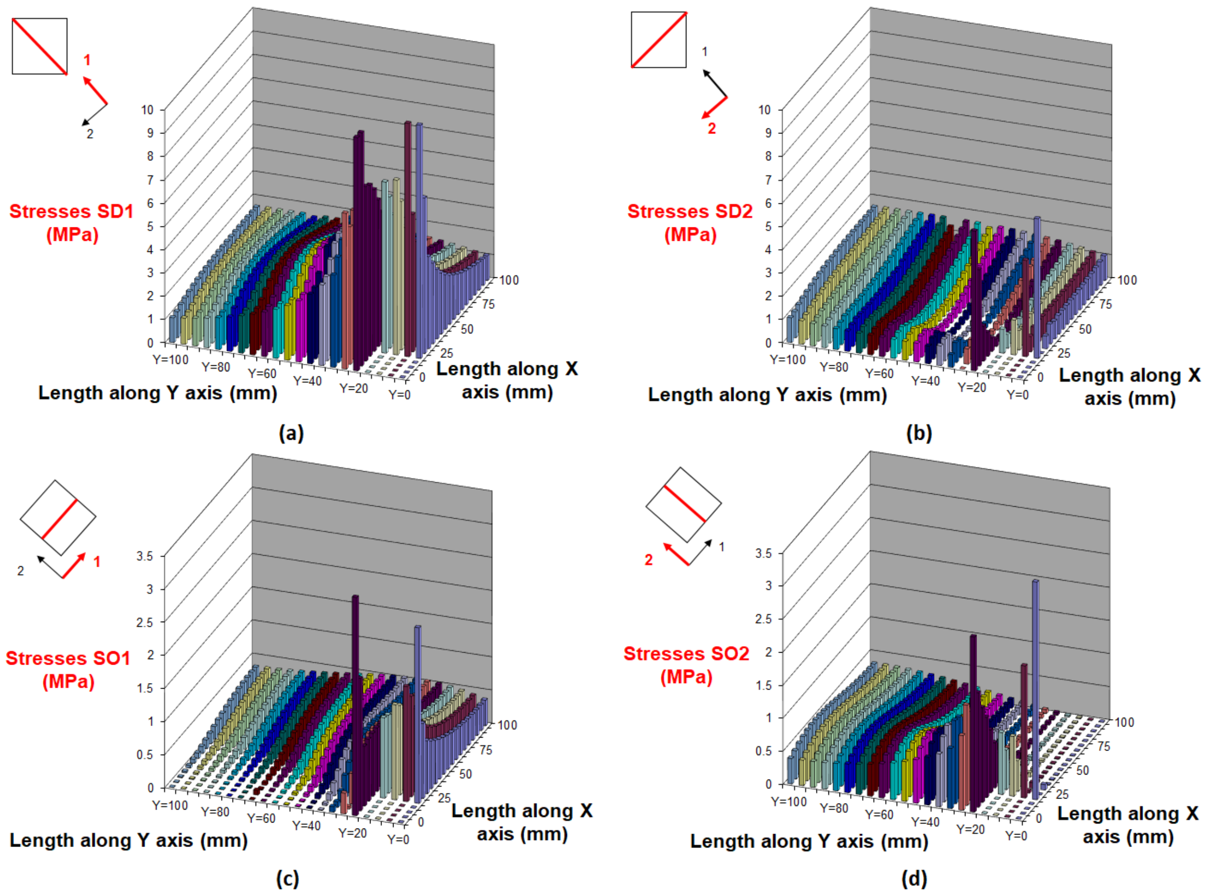

Fig. 2. Confining stresses in a quartile of a square section 200×200mm: along diagonal (top) and orthogonal (bottom) direction. The round corner stresses are not included.

Observing the plots above (Fig. 2), the following important remarks can be made:

- No unconfined concrete regions are observed, as assumed in many models. The central parts near the sides are confined from forces coming from the corners and moving parallel to the sides.
- The confining forces near the perimeter have strong directionality (uniaxial confinement) and on the other hand near the center there is more uniformity (biaxial confinement)

Within some tolerance, the regions where a biaxial and a uniaxial confinement exist can easily be identified, based on the ratio of the principal stresses of the two directions in the joints of the FEM (ratio of confining stresses less than 15%). It has been observed that the size of the biaxial stress state region is independent of the FRP stiffness; moreover, the radius of the rounded corner is affecting more the diagonal dimension of this region, while parallel to the sides the size remains the same. According to these results, the width of the uniaxially confined peripheral region can be simply calculated as 1/8 of the corresponding side (Figure 3). The dimensions of the regions are easily then related and determined according to this size.

3 SIMPLIFIED MECHANICAL MODEL

A series of “generalized” springs (Fig. 3) is used to describe the following confining behaviour. Compressed concrete expands laterally according to its confinement state. Such expansion activates the confining device.

The confining forces are applied at the section corners and directed along the diagonal (on passing, the resultant is always at 45° angle, regardless of the section aspect ratio). The figure below (Fig. 3) illustrates how the springs are modelling the vertical and the lateral behaviour of the section. In the vertical behaviour, the springs are experiencing the same vertical displacements and their strength is added (parallel system). In the lateral behaviour, the springs are experiencing the same force and their displacements are added (series system).

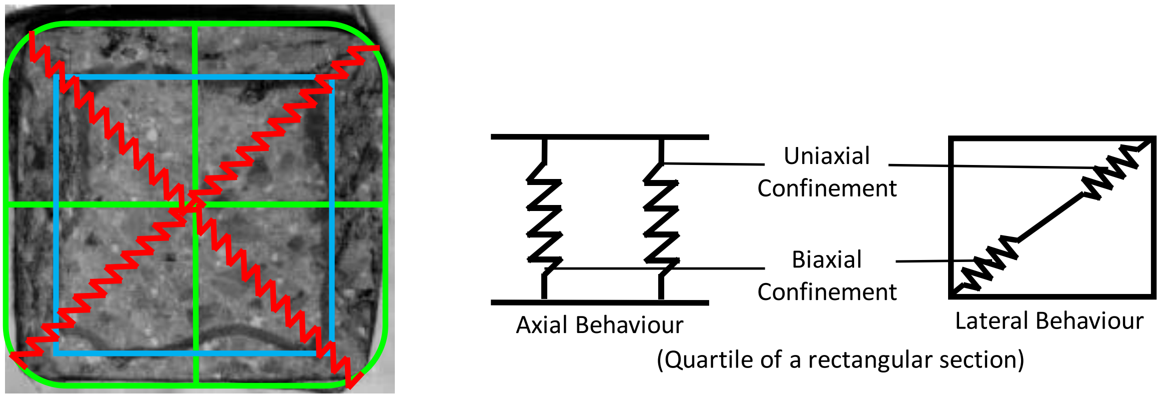

Fig. 3. FRP-confined rectangular concrete section modelling using ‘generalized’ springs.

For the constitutive law used to describe the behaviour of these “generalized springs”, the model of Pantazopoulou and Mills [5], which relates volumetric strains ε_V to axial strains ε_C, has been taken as a basis. In order to comply with the mechanical model of the “generalized” springs and the differently confined regions, that model has been modified so to relate volumetric strains ε_V to axial stresses σ_C instead, according to the following equation (the same linear-parabolic behaviour of volumetric strains versus axial strains has been experimentally observed between volumetric strains and axial stresses, as well):

$$\varepsilon_V = -(1-3\nu)\cdot 10^{-4}\cdot\sigma_c \qquad \sigma_c \le \alpha\, f_{co} \tag{1a}$$

$$\varepsilon_V = -(1-3\nu)\cdot 10^{-4}\cdot b\cdot f_{co}\left[\frac{\sigma_c}{b\,f_{co}} - \left(\frac{\sigma_c - \alpha\, f_{co}}{b\,f_{co} - \alpha\, f_{co}}\right)^c\right] \qquad \sigma_c > \alpha\, f_{co} \tag{1b}$$

The above equations describe the following behaviour. Initially, volume change is of compaction and is almost linear up to the critical stress of $\alpha \cdot f_{c0}$ (unconfined concrete strength, usually with α = 0.7). Note that for this axial stress level the Poisson’s ratio ν remains in the range of 0.15 - 0.25 (here, the initial Young’s modulus of concrete is usually determined, as well). At this point, volume change is reversed resulting in a volumetric expansion, called (near- or at-peak-strength) dilatancy. A point can be found where the compression rate of the specimen equates the expansion rate, thus resulting in zero volumetric strain. This point is considered to appear when the ultimate strength of the uniaxially confined region is reached (biaxial stress state, b = 1.2). After the deterioration of this region, the expansion rate increases more than the compression rate (second order parabola, c = 2) due to less effective confinement. The expansion becomes unstable during the crushing phase beyond the peak strength.

From volumetric strains, both area strain ε_A and side strains ε_a and ε_b can be easily calculated as follows (compressive axial strains are taken as negative, and a and b are the sides length, related by: $b/a = \tan\theta$, with θ is the diagonal angle):

$$\varepsilon_A = \varepsilon_V - \varepsilon_c \tag{2}$$

$$\varepsilon_A = \frac{\Delta A}{A} = \frac{(a+\Delta a)\cdot(b+\Delta b) - a\cdot b}{a\cdot b} = \frac{(a+\varepsilon_a\cdot a)\cdot(b+\varepsilon_b\cdot b) - a\cdot b}{a\cdot b} = (1+\varepsilon_a)\cdot(1+\varepsilon_b) - 1 \tag{3}$$

$$\frac{\varepsilon_a}{\varepsilon_b} = \frac{\Delta_a}{a}\frac{b}{\Delta_b} = \frac{\Delta_{diag}\cdot\cos\theta\cdot b}{\Delta_{diag}\cdot\sin\theta\cdot a} = 1 \quad\Rightarrow\quad \varepsilon_{side} = \varepsilon_a = \varepsilon_b \tag{4}$$

$$\varepsilon_A = (1+\varepsilon_{side})^2 - 1 \quad\Rightarrow\quad \varepsilon_{side} = \sqrt{\varepsilon_A + 1} - 1 \tag{5}$$

By the usual no-slip assumption between FRP jacket and concrete, side strains ε_a, ε_b and jacket strain can be equated. Thus, the diagonal force of the jacket applied from the corners to the springs can be determined as:

$$F_{diag} = \sqrt{2}\cdot E_j\cdot\varepsilon_{side}\cdot t_j\cdot k_e \tag{6}$$

$$k_e = \frac{R}{a}\cdot\frac{1}{2}\cdot\left(1+\frac{a}{b}\right) \tag{7}$$

where k_e is an efficiency factor by Karam and Tabbara [6], which considers that confinement effectiveness increases as the corner radius increases, and decreases as the aspect ratio of the section changes from square. Having determined the diagonal force applied from the corners to the lateral springs in series, the lateral pressures (assumed as uniform) for each region can be determined (Fig. 4). Two regions are identified: one with a triaxial stress state and one with a biaxial stress state. Note that no unconfined regions are to be found.

Based on the lateral pressures calculated above, the corresponding vertical stress can be easily determined by the use of a biaxial or a triaxial stress-strain model corresponding to the confinement stress state of each region. The stress-strain model by Mander et al. [7] is used to describe the behaviour of the triaxial stress-state region. The model's equation of maximum vertical stress f_{cc} is not used in this case due to the fact that it describes the performance of uniform biaxial confining pressure. In order to comply with the above modelling of the triaxial stress-state region where the confining pressures are different in two directions (they are equal only in square sections), the failure criterion by Ottosen [8] is applied. For the biaxial stress-state region, the model for concrete under biaxial stress-state of Liu et al. [9] is used. Finally, based on the areas of the different regions, the total averaged vertical stress of the section is calculated.

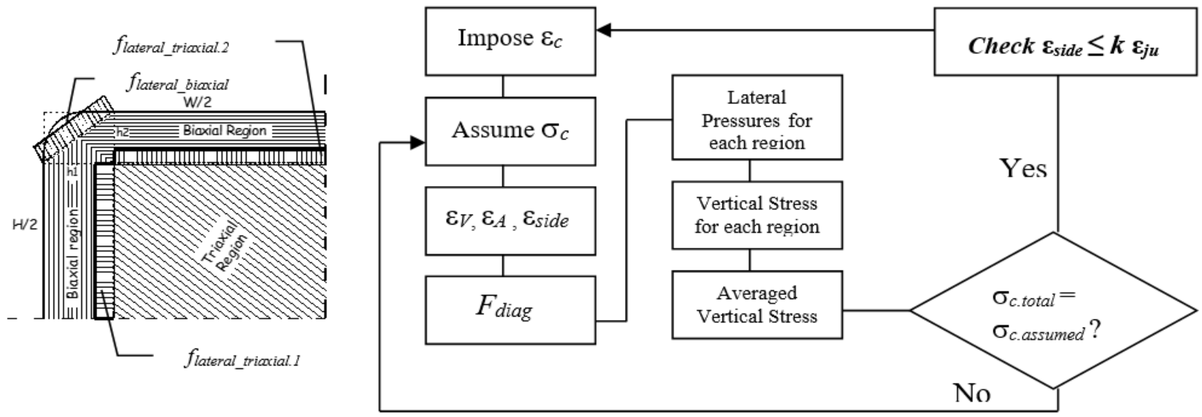

Fig. 4. Confining pressures in the regions – Iterative procedure.

An iterative procedure is proposed in Fig. 4, where an assumed value of axial stress σ_c corresponding to an imposed axial strain ε_c is brought to convergence. After convergence is reached between the assumed axial stress and that calculated with the above considerations, the resulting sides′ strain through the iterative procedure should be compared to the ultimate rupture strain of the jacket. It has been observed from experimental results [10] that the average failure strains of the FRP wraps are of the order of 50% - 80% of the failure strain of the tensile coupons made from the same material and tested before the application of the material. The value of factor *k* (ranging between 50% - 80%) depends on the type of FRP used.

4 ASSESSMENT AGAINST EXPERIMENTAL RESULTS

Recent experimental data collected by large-scale tests on FRP-confined rectangular RC columns [11] were used for the simulation of monotonic loading. Zeng *et al.* [11] presented the test results of an experimental study consisting of nine large-scale rectangular RC columns with a cross-section of 435mm in depth and 290mm in width, including eight FRP-confined RC columns and one RC column without FRP jacketing as the control specimen, tested under axial compression. The experimental program examined the sectional corner radius and the FRP jacket thickness as the key test variables. The proposed algorithm was assessed against three of these specimens, *i.e.* the specimens with corner radii 25mm or 45mm and one or two layers of Carbon Fiber Reinforced Polymer (CFRP) wrap. The corner radius of 65mm was not considered in the assessment, since in buildings designed using obsolete design codes the concrete cover thickness is typically small. Hence, a cover of at least 65mm which would allow the formation of the round corners in such a column is highly unlikely to be found.

Fig. 5 shows the correlation of the proposed material model with these experimental results and overall the numerical response can be characterized as satisfactory. It should be noted that for this comparison the iterative procedure was terminated for FRP rupture strain equal to 50% of that of the experimentally tested tensile FRP coupons [11].

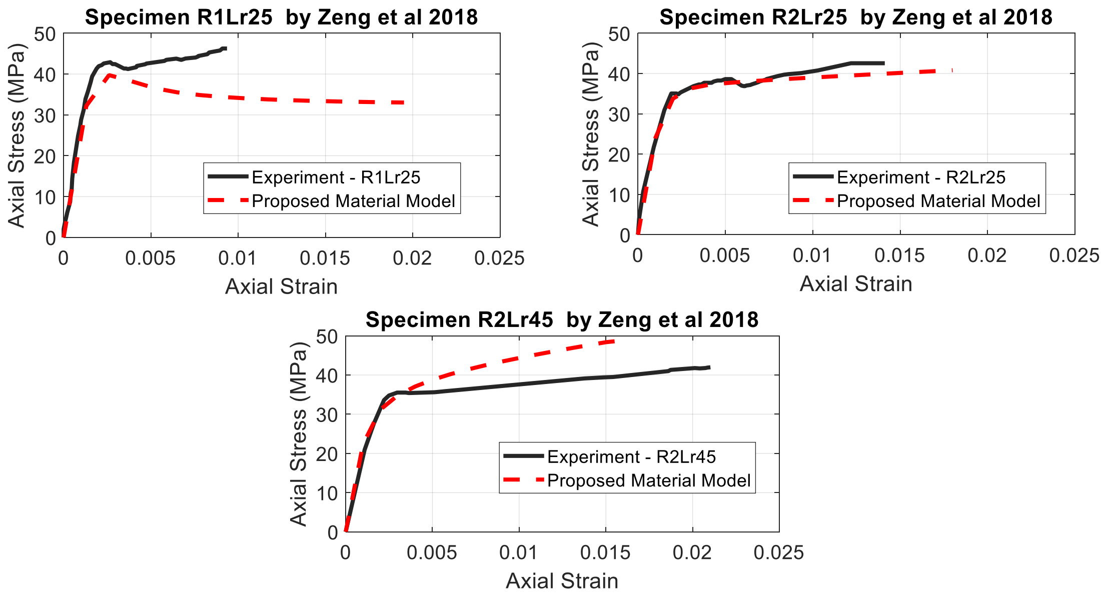

Fig. 5. Correlation of the proposed material model with experimental results of large-scale CFRP-confined rectangular RC columns under axial compression [11].

A further evaluation of the model's performance under cyclic lateral loading which simulates earthquake loads and simultaneous constant axial compression was performed. This was achieved by comparison against the experimental tests of FRP-retrofitted square RC columns performed by Memon and Sheikh [1]. This experimental study evaluates the effectiveness of Glass Fiber Reinforced Polymer (GFRP) wraps in strengthening deficient and repairing damaged square RC columns. Each of the eight specimens tested, representing columns of buildings and bridges constructed before 1971, consisted of a 305×305×1473mm column connected to a 508×762×813mm stub. Specimens were tested under constant axial compression and cyclic lateral displacement excursions simulating earthquake loads.

The modelling of these FRP-confined square RC columns has been performed using the MatLab toolbox FEDEAS lab ‘Finite Elements for Design Evaluation and Analysis of Structures’ [12]. The experimental moment-curvature responses within the plastic hinge regions are reported along with the numerical results in Fig. 6. The simulation of the cantilever columns has been applied using a unique fiber beam-column element [13] with force formulation for the entire column, in which the FRP-confined concrete was modelled using the proposed material model with degraded linear unloading/reloading stiffness according to the work of Karsan and Jirsa [14] and no tensile strength. The constitutive model by Menegotto and Pinto [15] is used to model the longitudinal steel behaviour. The moment-curvature response of the most critical fiber section of the applied nonlinear fiber element was then reported. It can be seen that the agreement is very close to the experimental one, with some deviation concentrated on the parts of reloading after reversal of the imposed displacement. This difference in response in terms of modelling can be explained based on the way the cracks on the concrete surface are described in the level of the material model. Because the crack is described as a two-event phenomenon (open or closed cracks), when the longitudinal steel reinforcement is in compression and the crack is closing, the concrete contributes to the total strength of the column, creating this deviation in the response. In reality, this is not the case due to imperfect crack closure.

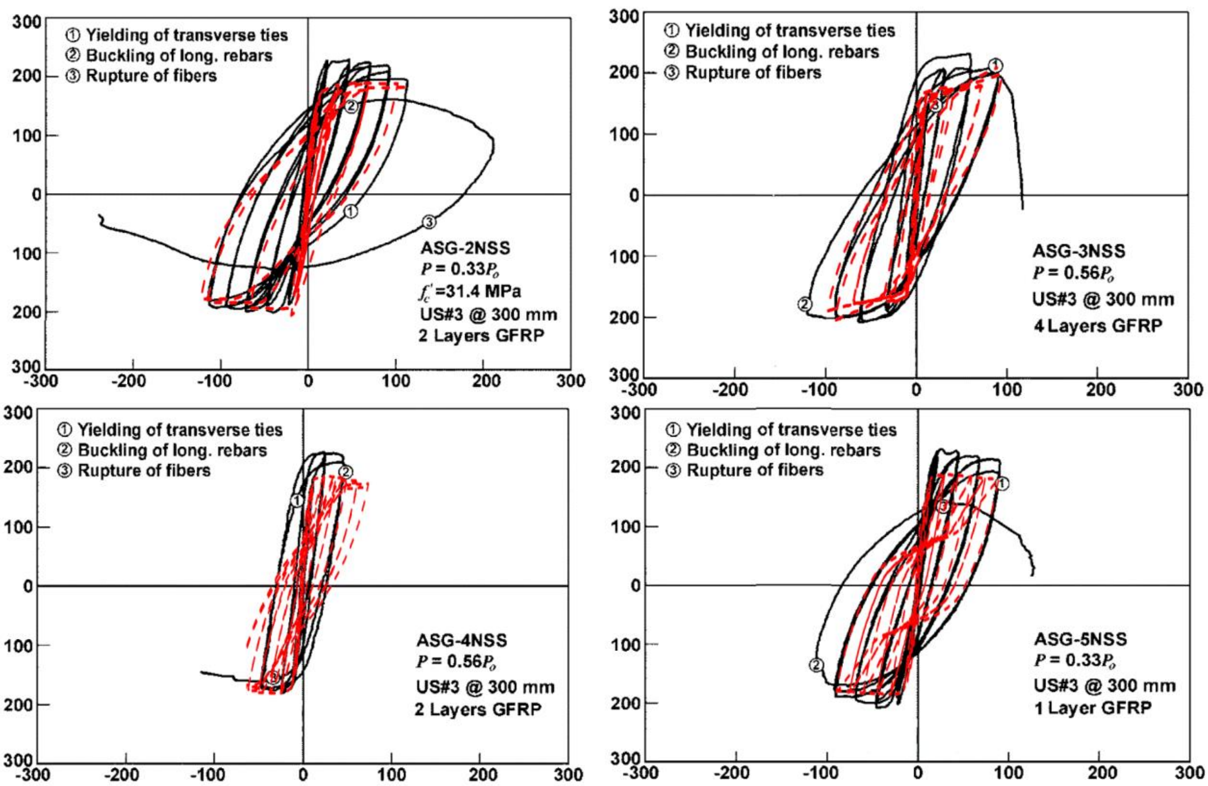

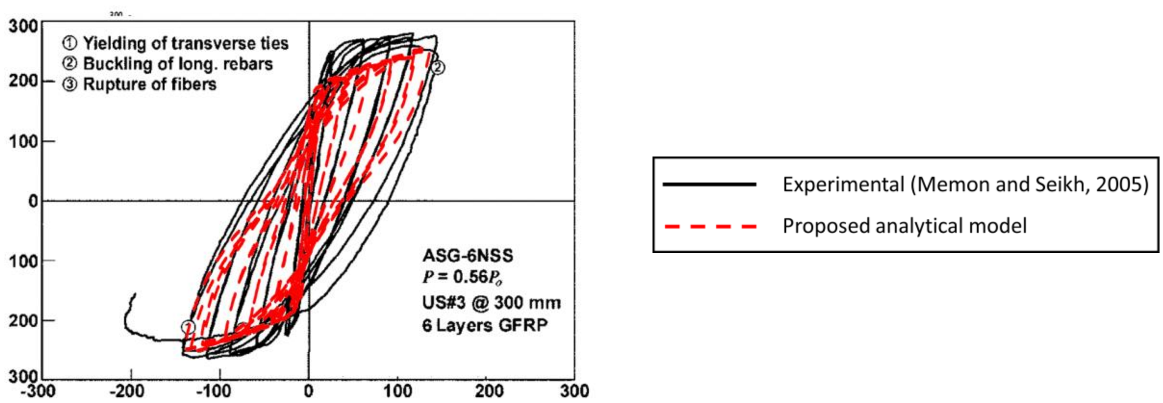

Fig. 6. Correlation of the proposed material model with experimental results of large-scale GFRP-confined square RC columns under cyclic excitation by Memon and Sheikh (2005) [1].

5 CONCLUSIONS

An iterative approach was proposed to model both the axial and lateral stress-strain response of axially loaded FRP-confined rectangular and square reinforced concrete columns.

In FRP-confined square or rectangular sections, no unconfined concrete regions are observed, as assumed in many models. These sectors along the sides between adjacent corners are confined from forces coming from the corners and moving parallel to the sides. Therefore, the areas where arching effect is assumed in the section are actually partially confined, so they contribute to the column’s total strength until their maximum strength (which is lower than the inner part of the section). Thus, two different regions with different confining stress-states are identified.

The two regions are uniaxially and biaxially confined (biaxial and triaxial stress-state, respectively). Therefore, the contribution of each region to the total section strength can be modelled as a system of parallel springs, whose axial stresses are added based on the corresponding constitutive law under biaxial or triaxial stress state.

The lateral behaviour develops along the diagonals of the section and can be represented by a system of springs in series. It was shown that both sides’ lateral strains in the rectangular sections are equal, regardless of their aspect ratio. The reacting force of the confining device applied from the corners can be shared among the regions based on the defined path of the confining forces and the geometry of the regions. The resulting lateral uniform pressures lead to the corresponding axial strength of the regions.

The algorithm takes into account all parameters available to designers, such as corner rounding radius, stiffness of the FRP and concrete strength, while it can be easily understood and implemented. Its results are found to correlate adequately to recent experimental data yielded by large-scale tests on FRP-confined rectangular RC columns. Finally, the performance of this material model was further investigated by its implementation to the simulation of a series of experimental tests of FRP-retrofitted square RC columns under cyclic lateral loading simulating earthquake loads and simultaneous constant axial compression. In particular, all specimens were simulated using nonlinear fiber elements, in which the FRP-confined concrete was modelled using the developed material model. Comparison between the numerical and experimental hysteresis of the column is indicative of the effectiveness of the implemented modelling.

REFERENCES

[1] Memon, M. S., Sheikh, S. A. (2005). Seismic resistance of square concrete columns retrofitted with glass fiber-reinforced polymer. *ACI structural journal, 102*(5), 774-783. DOI: 10.14359/14673

[2] Campione, G., Miraglia, N. (2003). Strength and strain capacities of concrete compression members reinforced with FRP. *Cement and Concrete Composites, 25*(1), 31-41. DOI: 10.1016/S0958-9465(01)00048-8

[3] Computers and Structures, Inc. 2016. CSI Analysis Reference Manual. Berkeley, CA: Taylor & Francis.

[4] Megalooikonomou K.G. & Papavasileiou, G.S. (In press). Analytical Stress-Strain Model for FRP-Confined Rectangular RC Columns. Submitted to *Frontiers in Built Environment – Earthquake Engineering***.**

[5] Pantazopoulou, S. J., Mills, R. H. (1995). Microstructural aspects of the mechanical response of plain concrete. *Materials Journal*, *92*(6), 605-616. DOI: 10.14359/9780

[6] Karam, G., Tabbara, M. (2005). Confinement effectiveness in rectangular concrete columns with fiber reinforced polymer wraps. *Journal of composites for construction*, *9*(5), 388-396. DOI: 10.1061/(ASCE)1090-0268(2005)9:5(388)

[7] Mander, J. B., Priestley, M. J. N., Park, R. (1988). Observed stress-strain behavior of confined concrete. *Journal of structural engineering*, *114*(8), 1827-1849. DOI: 10.1061/(ASCE)0733-9445(1988)114:8(1827)

[8] Ottosen, N. S. (1977). A failure criterion for concrete. *American Society of Civil Engineers. Engineering Mechanics Division. Journal*, *103*(4), 527-535.

[9] Liu, T. C., Nilson, A. H., & Slate, F. O. (1972). Biaxial stress-strain relations for concrete. *Journal of the Structural Division*, *98*(5), 1025-1034.

[10] Lam, L., Teng, J. G. (2003). Design-oriented stress-strain model for FRP-confined concrete in rectangular columns. *Journal of reinforced plastics and composites*, *22*(13), 1149-1186. DOI: 10.1177/0731684403035429

[11] Zeng, J. J., Lin, G., Teng, J. G., Li, L. J. (2018). Behavior of large-scale FRP-confined rectangular RC columns under axial compression. *Engineering Structures*, *174*, 629-645. DOI: 10.1016/j.engstruct.2018.07.086

[12] Filippou, F. C., Constantinides, M. (2004). FEDEASLab getting started guide and simulation examples. *NEESgrid Report*, *22*, 2004-05.

[13] Spacone, E., Filippou, F. C., Taucer, F. F. (1996). Fibre beam–column model for non-linear analysis of R/C frames: Part I. Formulation. *Earthquake Engineering & Structural Dynamics*, *25*(7), 711-725. DOI: 10.1002/(SICI)1096-9845(199607)25:7<711::AID-EQE576>3.0.CO;2-9

[14] Karsan, I. D., Jirsa, J. O. (1969). Behavior of concrete under compressive loadings. *Journal of the Structural Division*. 95(12):2543–64.

[15] Menengotto, M. (1973). Method of Analysis for Cyclically Loaded Reinforced Concrete Plane Frames Including Changes in Geometry and Nonelastic Behavior of Elements under Combined Normal Force and Bending. In *IABSE Symposium on Resistance and Ul-*

timate Deformability of Structures Acted on by Well-Defined Repeated Loads, Final Report, Lisbon, Portugal.